PHILOSOPHICAL TRANSACTIONS OF THE ROYAL SOCIETY B BIOLOGICAL SCIENCES

Magic Angle Sample Spinning in Inhomogenously Broadened Biological Systems

J. Herzfeld, A. Roufosse, R. A. Haberkorn, R. G. Griffin and M. J. Glimcher

Phil. Trans. R. Soc. Lond. B 1980 **289**, 459-469
doi: 10.1098/rstb.1980.0064

Phil. Trans. R. Soc. Lond. B **289**, 459–469 (1980) [459]
Printed in Great Britain

Magic angle sample spinning in inhomogeneously broadened biological systems

By J. Herzfeld†, A. Roufosse‡, R. A. Haberkorn§, R. G. Griffin and M. J. Glimcher‡

Francis Bitter National Magnet Laboratory, Massachusetts Institute of Technology, Cambridge, Massachusetts 02139, *U.S.A.*

† *Biophysical Laboratory, Harvard Medical School, Boston, Massachusetts* 02115, *U.S.A.*

‡ *Department of Orthopaedic Surgery, Harvard Medical School, Boston, Massachusetts* 02115, *U.S.A.*

Recent advances in magic angle sample spinning experiments now permit observation of dilute spin high resolution n.m.r. spectra of arbitrary powder samples. In the 'slow-spinning' régime, for which the spinning rate is less than the size of the interaction that is being averaged, the spectra exhibit rotational side bands whose intensities contain information on chemical shift anisotropies. A technique for extracting shift anisotropies from side band intensities is discussed. Since many biologically interesting systems are solid or semi-solid in nature, this technique should find wide application to biological systems. Two illustrations of the point are given in this paper, namely, n.m.r. studies of membranes and of the phosphate-containing phases of bone.

1. Introduction

Although there are many biological samples that yield high resolution n.m.r. spectra, there is, at the same time, a large class of systems that do not. In this latter category are biological membranes, bone and other systems in which there exists either anisotropic molecular motion or which exhibit rigidity, or near rigidity, on a microscopic scale. Proton n.m.r. spectra of such systems are strongly dipolar broadened and spectra of dilute spins (from ^{13}C, ^{31}P etc.) are broadened by dipolar interactions with nearby protons and also by chemical shift anisotropy effects. Thus, in the past, n.m.r. spectra of such systems have been considered intractable. The purpose of this paper is to discuss one means of regaining high resolution spectra in such instances; this involves combination of magic angle sample spinning (m.a.s.s.) with dilute spin double resonance techniques. We choose to concentrate on this approach since it shows promise of applicability to a wide variety of chemically and biologically interesting problems. We begin with a brief review of the development of the m.a.s.s. and dilute spin double resonance methods. Next, we consider recent advances in this field, including methods for obtaining chemical shift anisotropies from rotational side band intensities. Finally, we illustrate two applications of this technique with recent work, from this laboratory, on ^{13}C spectra of membranes and the $^{31}PO_4$-containing mineral phases of bone.

2. Magic angle sample spinning and dilute spin double resonance

The first attempts to obtain high reolution n.m.r. spectra of solid samples involved m.a.s.s.; these attempts were reported by Andrew *et al.* (1958) and by Lowe (1959). Briefly, the sample is spun rapidly about an axis inclined at the magic angle (54° 44′) with respect to H_0. In the

§ Present address: Laboratory for Physical Chemistry, ETH, CH-8092 Zurich, Switzerland.

limit that the spinning rate, ν_R, is greater than $\Delta\sigma$, the size of the chemical shift anisotropy, which is the interaction of primary interest here, the Hamiltonian becomes

$$\mathscr{H}_{c.s.} = \gamma\hbar H_0 I_z[\sin^2\beta\tfrac{1}{2}\mathrm{tr}\,\sigma_{ii} + \tfrac{1}{2}(3\cos^2\beta - 1)\sum_i \sigma_{ii}\cos^2\theta_i], \quad (1)$$

where $\hbar$, γ, H_0, I_z have their usual meaning, σ_{ii} are the principal values of the shielding tensor, θ_i specifies the orientation of the σ_{ii} to the rotation axis, and β is the angle between the rotation axis and the laboratory field, H_0. Clearly, when $\cos^2\beta = \frac{1}{3}$ then the anisotropic part of $\mathscr{H}_{c.s.}$ vanishes and one obtains a 'high resolution' n.m.r. spectrum. In the original and much subsequent work, the interaction that was the object of the spinning experiment was static dipolar broadening (denoted by Δ), which can be substantially larger (*ca.* 20–50 kHz) than easily obtainable spinning rates (*ca.* 5 kHz). Thus, because of the restriction $\nu_R > \Delta$, the technique has been successfully applied only to systems with inherently narrow static linewidths (Andrew 1971).

The early 1970s witnessed the development of several pulse methods for obtaining high resolution spectra of strongly coupled dipolar solids, and, concurrently, the development of ^{13}C liquid state spectroscopy. Together, these advances generated thought as to how high resolution ^{13}C spectra of solids might be obtained; this question was answered in a general fashion by Pines *et al.* (1973). Because of their low magnetic moment and isotopic abundance, ^{15}C nuclei in solids constitute a magnetically dilute spin reservoir, with the consequence that homonuclear dipolar interactions are much reduced. Thus, in the absence of heteronuclear dipolar broadening, high resolution spectra can be obtained by direct observation of the ^{13}C signals. Of course, in general, heteronuclear broadening is present and in rigid solids the ^{13}C T_1 can be excruciatingly long. However, both of these problems can be circumvented with use of sufficiently intense decoupling fields and by cross polarization of the dilute spins with protons via a Hartmann-Hahn contact. This technique is generally applicable to any system that contains abundant and dilute spins, and has been used to examine a large variety of nuclei. For a single crystal, one observes narrow line spectra, which can be studied as a function of orientation to obtain, for instance, chemical shift (Herzfeld *et al.* 1978) and quadrupolar and dipolar tensors (Stark *et al.* 1978). However, when powdered or amorphous samples are investigated, anisotropic powder line shapes are observed, and, when there is more than one chemical shift, these often overlap and become difficult if not impossible to analyse. In 1976 Schaefer & Stejskal (1976) demonstrated a means to overcome this problem, when they showed that high resolution isotropic ^{13}C spectra of solid polymers could be obtained by combination of m.a.s.s. with dilute spin double resonance, This experiment was expected to work because the breadth of ^{13}C shift tensors (in hertz) at low fields ($\leqslant 2.0$ T) is comparable to practically obtainable spinning rates. Furthermore, it was thought, based on our naive understanding of the dipolar case, that the experiment would be limited to low fields, since at higher fields, $\Delta\sigma$, the breadth of shift anisotropy powder patterns, can greatly exceed ν_R. However, it was reported by Lippmaa *et al.* (1976) and subsequently by others (Stejskal *et al.* 1977; Maricq & Waugh 1977; Haberkorn *et al.* 1978) that these expectations are not correct. Specifically, powder patterns associated with inhomogeneous interactions, such as the chemical shift, break up into sharp spinning side bands at $\nu_R < \Delta\sigma$. An illustration of this point is given in figure 1, which shows ^{31}P spectra of barium diethylphosphate, $Ba(PO_4(C_2H_5)_2)_2$ (BDEP), as a function of ν_R. At $\nu_R = 0$ we observed an axially asymmetric powder spectrum of *ca.* 22 kHz total breadth at our 6.8 T field. Upon spinning at *ca.* 1, 2 and 3 kHz, the powder pattern breaks up into a series of rotational sidebands

PHILOSOPHICAL TRANSACTIONS OF THE ROYAL SOCIETY B BIOLOGICAL SCIENCES

spaced at ν_R and symmetrically disposed about a centre band (marked with a dashed line) at the isotropic resonance frequency. The physical explanation of this phenomenon, which involves formation of mechanically induced spin echos (Carr 1953), has been discussed elsewhere (Waugh *et al.* 1978).

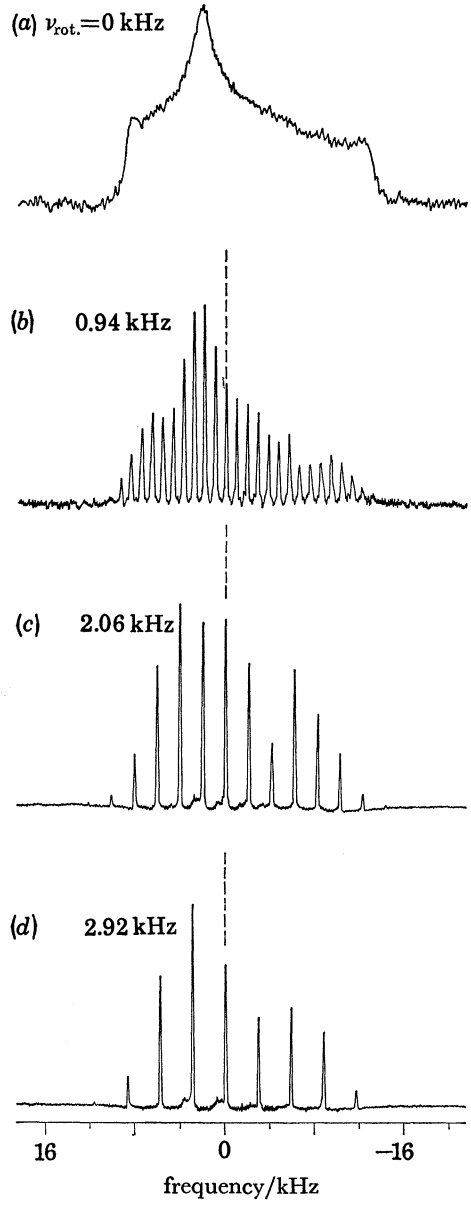

FIGURE 1. ^{1}H decoupled ^{31}P m.a.s.s. spectra of BDEP. The powder pattern in (*a*) is *ca.* 23 kHz wide and narrows to a spectrum exhibiting side bands of 60 Hz full width at ν_R = 2.92 kHz. The dashed line marks the isotropic shift. $\nu_{^{31}P}$ = 119.05 MHz.

It can be discerned from figure 1 that the side band intensities contain information on the shift anisotropy, which could be used for a variety of purposes, e.g. identification, studies of anisotropic molecular motion etc., if it could be extracted. Maricq & Waugh (1979) have proposed a moment analysis to obtain these data. Specifically, for an $I = \frac{1}{2}$ system, the second and third moments are sufficient to determine the shift anisotropy. Lippmaa *et al.* (1976) have

PHILOSOPHICAL TRANSACTIONS OF THE ROYAL SOCIETY B BIOLOGICAL SCIENCES

calculated the intensities of the centre band and of the first two side bands for an axially symmetric tensor in the limit $\nu_0\delta/2\nu_R < 1$, where $\delta = \sigma_{33} - \frac{1}{3}\mathrm{Tr}\,\sigma$. Unfortunately, most shift tensors are not axially symmetric and at high fields the limit $\nu_0\delta/2\nu_R < 1$ is difficult to achieve. We have extended the side band calculations of Lippmaa *et al.* to include all side bands and asymmetric chemical shift tensors. These calculations are rather lengthy and will be described completely elsewhere (Herzfeld & Berger 1980); here, we present a brief description of them and illustrate how they can be employed in shift tensor determinations. The intensity of the Nth side band is given by

$$I_N = \frac{1}{4\pi}\int_0^{\pi}\int_0^{2\pi} (T_1^2 + T_2^2)\,\mathrm{d}\alpha \sin\beta\,\mathrm{d}\beta, \tag{2}$$

where

$$T_1 + \mathrm{i}T_2 = \frac{1}{2\pi}\int_0^{2\pi} \exp(-\mathrm{i}\phi N)\exp\left[-\mathrm{i}\left(\frac{A_1}{\omega_R}\cos\phi + \frac{B_1}{\omega_R}\sin\phi + \frac{A_2}{2\omega_R}\cos 2\phi + \frac{B_2}{2\omega_R}\sin 2\phi\right)\right]\mathrm{d}\phi.$$

$$A_1 = \tfrac{2\sqrt{2}}{3}\{\tfrac{1}{2}\sin\beta\cos\beta[\Delta_+ + \cos(2\alpha)\Delta_-]\},$$

$$B_1 = \tfrac{2\sqrt{2}}{3}\{\tfrac{1}{2}\sin\beta\sin(2\alpha)\Delta_-\},$$

$$A_2 = \tfrac{2}{3}\{\cos\beta\sin(2\alpha)\Delta_-\},$$

$$B_2 = \tfrac{2}{3}\{\tfrac{1}{4}\sin^2(\beta)\Delta_+ - \tfrac{1}{4}(1+\cos^2\beta)\cos(2d)\Delta_-\},$$

$$\Delta_+ = (\sigma_{11} - \sigma_{33}) + (\sigma_{22} - \sigma_{33}), \quad \Delta_- = \sigma_{11} - \sigma_{22}$$

and α and β are Euler angles over which a powder average must be performed. This expression can be evaluated numerically for a given shift anisotropy and spinning rate, and we have found close agreement between measured and calculated side band intensities for BDEP. However, the above expression cannot be readily inverted to allow determination of the shift tensor from the I_N, but, it can be used to generate contour plots of I_N/I_0 for various values of N as a function of $\mu = (\sigma_{33} - \sigma_{11})/\nu_R$ and $\rho = (\sigma_{11} + \sigma_{33} - 2\sigma_{22})/(\sigma_{33} - \sigma_{11})$. The variables have been chosen because, for the conventional assignment of the principal values of the shift tensor, $\sigma_{11} < \sigma_{22} < \sigma_{33}$, $\mu > 0$ and $-1 < \rho < 1$ (the extremes corresponding to axially symmetric tensors). Figure 2*a*, *b* shows contour plots for $N = +5$ and -5, respectively; the dotted lines on the plots indicate the intensities of the $N = \pm 5$ side bands of BDEP for $\nu_R = 1.744$ kHz. By properly superimposing plots and finding the unique intersection point of the contours corresponding to different side bands (± 1, ± 3, ± 5), values for ρ and μ can be obtained; this is shown in figure 2*c*. From our single crystal study of BDEP, we expect $\rho = 0.37$ and $\mu = 12.7$; this is marked with a cross on figure 2*c*. Considering the coarseness of our present contour plots, we believe that the agreement is very good; obviously, a finer grid would improve the results. Note that due to the many possible values of the functions involved a pair of contours may intersect more than once. However, all lines must pass through the true values of ρ and μ.

3. Applications to biological systems

A. *Membranes*

Although, over the last decade, a great deal of effort has been expended in n.m.r. studies of model and biological membranes, these systems have been a source of frustration for the n.m.r. spectroscopist. In most biological membranes and in multilamellar model systems, the n.m.r. lines are very broad because of the semisolid nature of these systems. Thus, proton spectra are

PHILOSOPHICAL TRANSACTIONS OF THE ROYAL SOCIETY B BIOLOGICAL SCIENCES

broadened by incomplete averaging of homonuclear dipolar interactions and ^{13}C spectra, both by incomplete removal of heteronuclear dipolar coupling and by shift anisotropy effects. As a consequence, most n.m.r. studies have dealt, not with intact biological membranes or multilamellar model systems, but rather with small single bilayer systems produced by ultrasonic irradiation. Ultrasonic irradiation reduces the particle size and thus the reorientational correlation times, and dramatically improves the resolution of the n.m.r. spectra. However, the exact physical and chemical consequences of such treatment have been the subject of much debate (see Bloom *et al.* 1979 for a recent discussion). That is, it is thought by some that the small radius of curvature of vesicles may change the chemical and physical properties

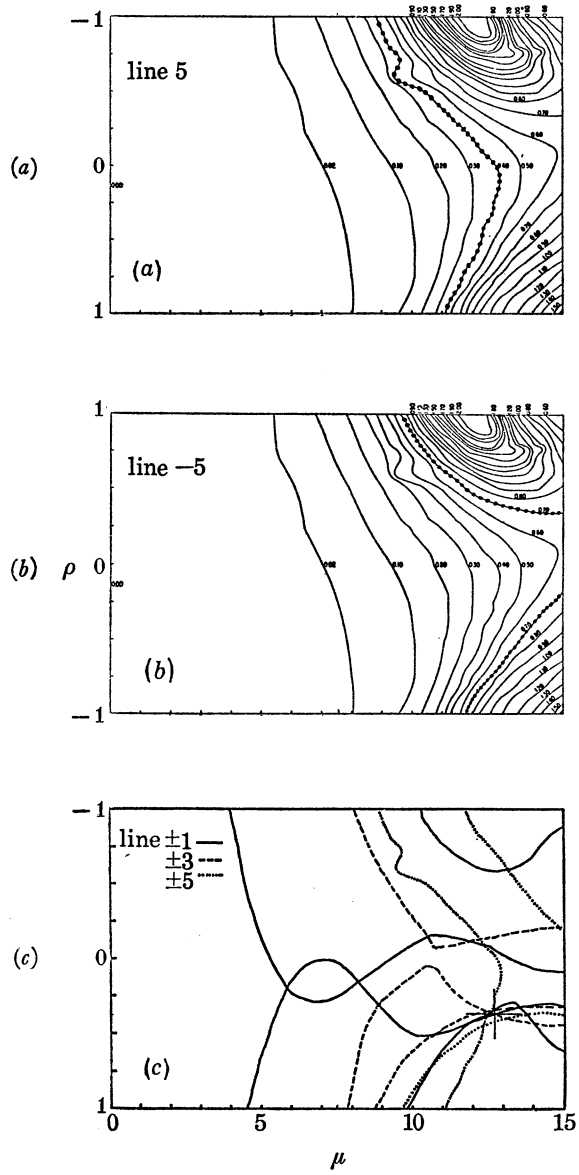

FIGURE 2. Contour plots for I_N/I_0 for (*a*) $N = +5$ and (*b*) $N = -5$. The dotted lines show I_N/I_0 for BDEP at $\nu_R = 1.744$ kHz. (*c*) Summary of contours for I_N/I_0, $N = +1, \pm 3, \pm 5$, for BDEP at $\nu_R = 1.744$ kHz. The true values of ρ and μ are obtained from the point where all of the contours intersect. The expected intersection ($\mu = 12.7$, $\rho = 0.37$), derived from a single crystal tensor determination, is marked with a cross.

of the lipid bilayers relative to essentially planar arrays that occur in biological membranes and in multilamellar dispersions. However, even if it could be decided that sonication does not alter bilayer properties, there is another disadvantage to studying sonicated systems. Specifically, above T_c, the gel–liquid crystalline transition temperature, well resolved spectra are observed. However, when the temperature is lowered into the gel state, vesicle fusion occurs and the resolution is lost (Levine *et al.* 1972). Thus, if spectroscopy of gel state lipids is of interest, and it appears that in certain biological membranes regions of gel state and liquid crystalline state coexist (Stockton *et al.* 1977), then it would be desirable to have a spectroscopic technique capable of examining both. The combined m.a.s.s. double resonance experiments discussed above satisfy this requirement, as is illustrated in figure 3.

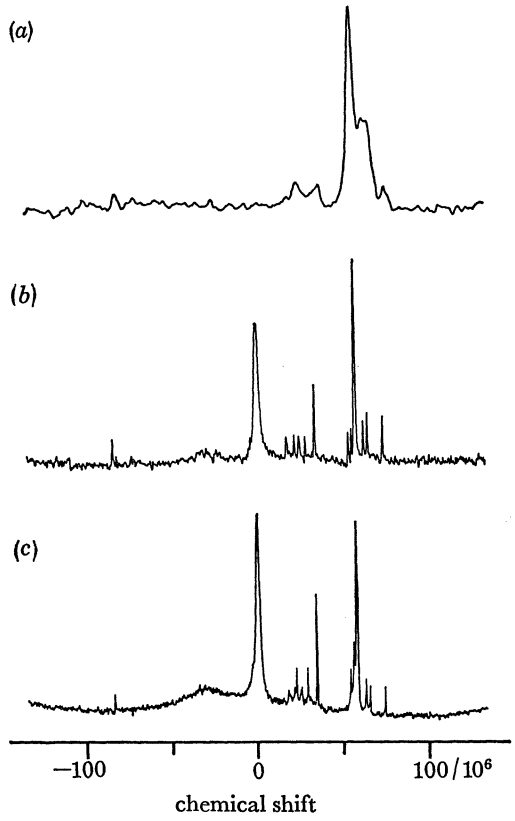

FIGURE 3. ^{1}H decoupled ^{13}C spectra of DMPC and DPPC in 50% (by mass) H_2O ($T \geqslant 21$ °C): (*a*) DMPC, $\nu_R = 0$; (*b*) DMPC, $\nu_R = 2.6$ kHz; (*c*) DPPC, $\nu_R = 2.6$ kHz. Line assignments are given in Haberkorn *et al.* (1978). Full widths of single carbon resonances are 20 Hz. The intense line at 0 chemical shift in (*b*) and (*c*) arises from ^{13}C in the plastic rotor, while the broad component at $-30/10^6$ is believed to come from Teflon insulation.

Figure 3*a* is a (properly) proton decoupled ^{13}C spectrum obtained from a stationary sample of dimyristoylphosphatidylcholine (DMPC); while bands of resonances corresponding to the various types of carbons in the molecule are discernible ($> C = 0$, $-CHO-$, $-CH_2-$ and $-CH_3$), this spectrum can hardly be called well resolved. However, upon spinning this sample at $\nu_R = 2.6$ kHz (figure 3*b*), we observe every resonance that is found when the lipid is dissolved in organic solvents. The strong line in the centre of the spectrum arises from the ^{13}C nuclei in

our plastic (Delrin) rotor. For DMPC, $T_c = 23.9°$ and, because of heating from the decoupling, we believe that spectrum 2*b* is due to liquid crystalline phase lipid. To observe a gel state spectrum, we examined dipalmitoylphosphatidylcholine (DPPC), which has $T_c = 41.4$ °C; its spectrum is shown in figure 3*c*. We note that there are some differences between these spectra, particularly in the glycerol region; these might arise from slightly different conformations in this part of the molecule above and below the phase transition temperature. Thus, it is now possible to obtain both liquid crystalline and gel state lipid spectra and, consequently, many membrane associated problems that have hitherto been inaccessible can now be studied.

B. *Bone*

Although there are significant uncertainties in our knowledge of the growth and maturation of bone and other calcified tissues, it is thought to proceed through what is *roughly* a two or three step process (Glimcher 1976). Initially, there exists a matrix containing organically bound phosphate, where nucleation occurs and a calcium phosphate mineral phase is formed. Until recently, the structure and composition of this initial mineral phase has been uncertain, as have been the transformations that it undergoes to form the final phase. Nevertheless, it is generally agreed that the final calcium phosphate phase that exists in mature tissues resembles hydroxyapatite, $Ca_{10}(PO_4)_6(OH)_2$ (HA) (Glimcher 1976). Evidence for this sequence of events is obtained by a number of approaches, including powder X-ray diffraction, electron optical techniques and wet chemical analysis. Unfortunately, these investigations have been hampered by a number of biologically and physically related problems.

The biological problems are associated with such things as specimen preparation and mineral phase heterogeneity inherent in the calcified tissues selected for study. As a result of these difficulties, there have been efforts to develop techniques for separating the various mineral phases of bone; one of the most successful has been density fractionation by means of differential centrifugation in organic solvents. With use of this technique, relatively homogeneous fractions, which can be used for physical studies, can be obtained (Roufosse *et al.* 1979).

In the past, the physical technique that has been most extensively employed in studies of calcified tissue has been X-ray diffraction. However, a number of factors, including the small size of calcium phosphate crystallites, lattice strains and the presence of more than a single phase, result in diffraction patterns exhibiting only a few broad, overlapping lines. Nevertheless, with X-rays it can be shown that the most mature mineral phase in bone is similar to synthetic, poorly crystalline HA; and recently, with homogeneous samples prepared by means of density fractionation, it was shown that brushite ($CaHPO_4 \cdot 2H_2O$) is probably the initial mineral phase deposited from the organic-phosphate matrix (Roufosse *et al.* 1979). However, with X-rays, brushite is only detected in the very earliest mineral phases and, thus, it is not known if significant amounts of this or other mineral phases exist in more mature tissue.

We have recently addressed the question of the composition and structure of bone mineral phases as a function of tissue maturation with ^{31}P m.a.s.s. experiments and we now present some of our results. We show first the futility of studying stationary powder samples of bone and then that we can differentiate, by rotational side band intensities, between two mineral phases known to exist in bone, e.g. HA and brushite. Finally, we have utilized this fact in an investigation of the maturation of bone tissue and we present evidence that the first mineral phase deposited is brushite, and that significant amounts of brushite coexist with HA in relatively mature tissue.

PHILOSOPHICAL TRANSACTIONS OF THE ROYAL SOCIETY B BIOLOGICAL SCIENCES

Figure 4 shows ^{31}P powder spectra obtained from high (greater than 1.8 g/cm^3) and from low (less than 1.8 g/cm^3) density fractions of bone and a spectrum of synthetic brushite for comparison. There are some differences among these spectra, for example, in the low density fraction there is a broad tail that is not present in the high density fraction. However, because of

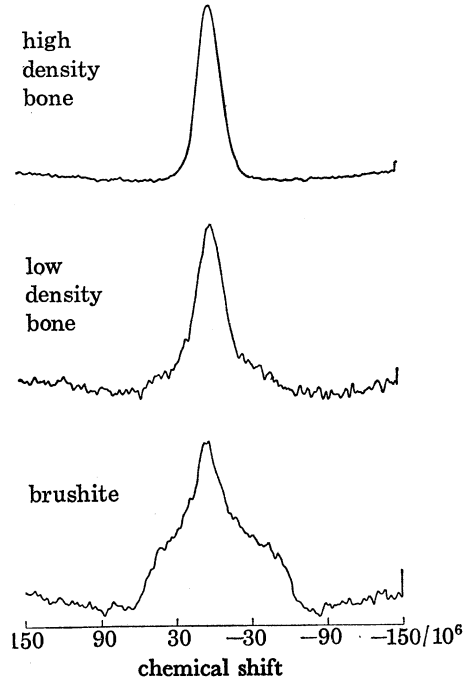

FIGURE 4. ^1H decoupled ^{31}P powder spectra of high density ($\rho > 1.8$ g/cm^3) and low density ($\rho < 1.8$ g/cm^3) bone and synthetic brushite ($CaHPO_4.2H_2O$).

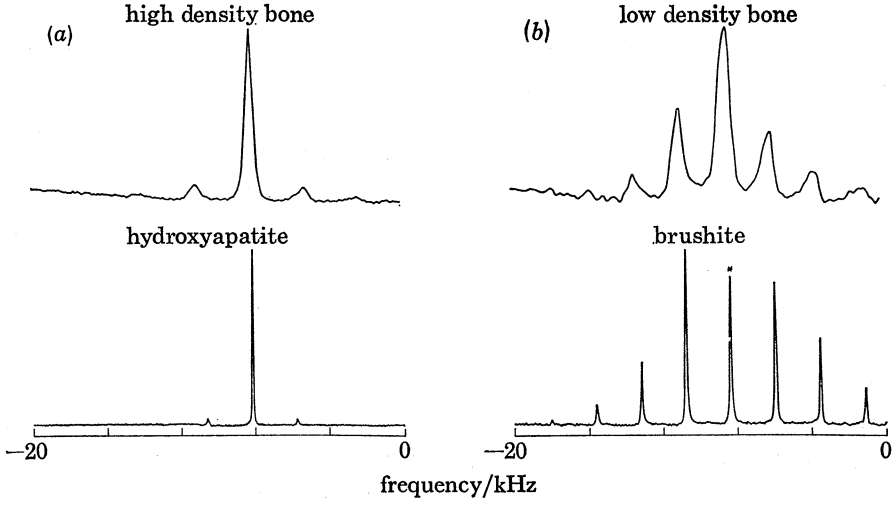

FIGURE 5. Comparison of ^1H decoupled ^{31}P m.a.s.s. spectra of the bone samples shown in figure 3 with synthetic standards: (*a*) high density bone and hydroxyapatite (HA); (*b*) low density bone and brushite. In each case the sideband intensities in the bone spectra compare favourably with those found in the synthetic samples. The asterisk marks the centre band in the brushite spectrum. Note the small shift differences between the centre bands in HA and brushite and in the bone samples. The increased line widths in the bone spectra are presumably due to a dispersion of shifts. The frequency scale is arbitrary.

spectral overlap and the fact that the composition is not known, it would probably be futile to attempt to extract quantitative information from them. Upon spinning these samples it becomes clear that the high density fraction is primarily HA, while the low density fraction contains a significant amount of brushite, as is shown in figure 5. Figure 5*a* shows the high density fraction; the intensities in the rotational side band pattern match very closely those obtained from a synthetic sample of HA; the same is true for the low density fraction when it is compared with a synthetic sample of brushite (figure 5*b*). We should note, however, that the centre band in 5*b*

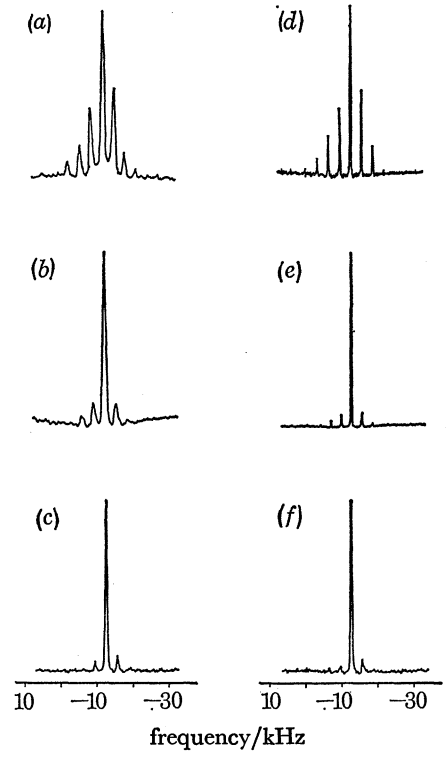

FIGURE 6. Comparison of ^{1}H decoupled ^{31}P m.a.s.s. spectra of bone tissues at increasing stages of development (*a–c*) and different mixtures of synthetic brushite and apatite (*d–f*): (*a*) earliest bone tissue deposits obtained in the density fractionation procedure of the diaphysis of tibiae from chicks 17 days embryonic, $\nu_R = 2.5$ kHz; (*b*) whole mid-diaphysis of tibiae of chicks 17 days embryonic, $\nu_R = 3.1$ kHz; (*c*) same as (*b*) but dissected from animals 5 weeks postnatal, $\nu_R = 3.0$ kHz; (*d*) mixture of brushite and apatite in the ratio 2 : 1 by mass, $\nu_R = 2.5$ kHz; (*e*) brushite apatite, 1 : 2, $\nu_R = 2.1$ kHz; (*f*) carbonato-apatite, $\nu_R = 3.0$ kHz, $\nu_{^{31}P} = 119.065$ MHz.

is more intense than it should be if the sample were pure brushite. This is because the density fractionation on these two samples was incomplete; undoubtably there is some HA remaining in the sample. There are three other points worth noting about these spectra. First, since the HA shift tensor is very narrow, its spectrum consist essentially of a centre band and, consequently, when rotational side bands are observed they cannot have arisen from HA. Thus, measurement of the side band intensities allows one to quantitate the amount of brushite present in mixtures that contain brushite and HA alone. Secondly, we note that the line widths in the bone samples are noticably larger than those observed in the synthetic samples. We have consistently observed this phenomena in bone and other calcified tissues and believe that it is due to the same factors that limit the resolution of X-ray diffraction, e.g. strains, impurities, lack of long range order etc., and which result in a dispersion of chemical shifts. Finally, there is a small

chemical shift difference (*ca.* $1.5/10^6$) between the centre band in synthetic HA and that in brushite; this difference is also observable in the high and low density, as well as other, bone samples. While measurement of isotropic shifts in these spectra is difficult because of the large line widths, the shift difference is, nevertheless, additional evidence that brushite and HA are indeed the mineral phases we observe.

Our success with these two samples encouraged us to apply the m.a.s.s. experiment to other problems. Partial results of one such experiment, designed to study mineral composition of bone as a function of age, are shown in figure 6. As mentioned above, it is thought that the initial mineral phase deposited is brushite, which undergoes a transformation to HA in mature bone, our experimental results seem to confirm this hypothesis. Figure 6*a* is a ^{31}P spectrum of the earliest bone tissue deposits obtained from density fractionation of the diaphysis of tibiae from chicks 17 days embryonic. In this spectrum ($\nu_R = 2.5$ kHz), strong rotational side bands are observed and their intensities correspond closely to those found in brushite. For comparison, we include in 6*d* a spectrum of a 2 : 1 (by mass) brushite–HA mixture. The spectra in figures 6*b* and 6*c* were obtained from progressively older tissue; the sample in 6*b* was the whole mid diaphysis of chick 17 days embryonic, while that in 6*e* is the same, except dissected, from an animal five weeks postnatal. In figure 6*b* we note that there are moderately strong side bands with intensity ratios (from left to right in the spectrum) of approximately 2:4:4:1; this is what is observed from brushite at this spinning frequency (3.1 kHz). Since HA yields only one pair of weak, equal intensity side bands at this frequency (see figure 5*a*), we conclude the side bands are due to primarily to brushite. We have observed spectra like this from a number of samples and, thus, have no doubt about the reproducibility of these side band intensities. However, the centre band position corresponds to HA and so both mineral phases are present. For comparison, we have included a spectrum of a 1:2 brushite–apatite mixture in figure 6*e*. It is worth mentioning that in this tissue, X-rays show only an apatite lattice, but, with n.m.r., we clearly observe the presence of both brushite and apatite. Figure 6*c* is a spectrum of the most mature tissue that we have investigated (an animal 5 weeks postnatal) and we note that the rotational side bands are now less intense and only one pair is present. We have been able to produce reasonable facsimiles of the spectrum with 1:5 brushite–apatite mixtures. However, another reasonable simulation can be obtained from carbonato-apatite (*ca.* 5% (by mass) carbonate replacing a phosphate), as is shown in figure 6*f*. At present we are investigating ways to differentiate between these alternatives.

Finally, we should note that, in our comparisons of synthetic and biological samples, we have used brushite and apatite samples exclusively. It is possible that other calcium phosphate phases are present in the mineral of bone and that their shift anisotropies could generate side band patterns similar to those obtained from brushite or apatite. However, we think this unlikely because other phases have not been detected by either X-rays or chemical analysis, and because other synthetic standards that we have examined fail to generate similar rotational side band patterns in ^{31}P m.a.s.s. spectra.

4. Conclusions

In summary, we have illustrated three main points in this paper. First, m.a.s.s. dilute spin double resonance experiments are capable of yielding high resolution n.m.r. spectra of powders and rotational side bands in these spectra can be employed to determine the principle values of

chemical shift tensors. Secondly, this technique can be employed to obtain well resolved spectra of membrane samples and, thus, the impediment to these studies that has existed for about a decade can now be circumvented. Finally, we have demonstrated the manner in which the presence (or absences) of side bands can be employed to identify the phosphate-containing phases of bone. In addition, we have identified brushite as the most probable initial mineral phase in bone and have shown that brushite persists in more mature bone tissue, but with apatite as the dominant calcium phosphate phase. As was mentioned in the Introduction, there is a large class of biological systems that are solid or semisolid in nature. Because this is so the n.m.r. technique discussed here will undoubtably find application in future investigations of these systems.

The research was supported by NSF grant C-670 to the Francis Bitter National Magnet Laboratory and by NIH Grants AM-15671, GM-23289 and GM-23316.

References (Herzfeld *et al.*)

Andrew, E. R., Bradbury, A. & Eades, R. G. 1958 *Nature, Lond.* **182**, 1659.
Andrew, E. R. 1971 *Prog. nucl. magn. Reson. Spectrosc.* **8**, 1–38.
Bloom, M., Burnell, E. E., MacKay, A. L., Nichol, C. P., Valic, M. I. & Weeks, G. 1979 *Biochemistry, N.Y.* **17**, 5750–5762.
Carr, H. Y. 1953 Ph.D. thesis, Harvard University.
Glimcher, M. J. 1976 *Handbook of physiology, endocrinology*, vol. 7, (ed. R. O. Greep & E. B. Astwood), p. 25. Washington: American Physiological Society.
Haberkorn, R. A., Herzfeld, J. & Griffin, R. G. 1978 *J. Am. chem. Soc.* **100**, 1296–1298.
Herzfeld, J., Griffin, R. G. & Haberkorn, R. A. 1978 *Biochemistry, N.Y.* **17**, 2711–2718.
Herzfeld, J. & Berger, A. M. 1980 (to be published).
Levine, Y. K., Birdsall, N. J. M., Lee, A. G. & Metcalfe, J. C. 1972 **11**, 1416–1421.
Lippmaa, E., Alla, M. & T. Tuherm 1976 *Proc. 19th Congress Ampere, Heidelberg*, pp. 113–118. Heidelberg and Geneva: Groupement Ampère.
Lowe, I. J. 1959 *Phys. Rev. Lett.* **2**, 285–287.
Maricq, M. & Waugh, J. S. 1977 *Chem. Phys. Lett.* **47**, 327–329.
Maricq, M. & Waugh, J. S. 1979 *J. chem. Phys.* **70**, 3300–3316.
Pines, A., Gibby, M. G. & Waugh, J. S. 1973 *J. chem. Phys.* **59**, 569–590.
Roufosse, A. H., Landis, W. J., Sabine, W. K. & Glimcher, M. J. 1979 *J. Ultrastruct. Res.* **68**, 235–255.
Schaefer, J. & Stejskal, E. O. 1976 *J. Am. chem. Soc.* **98**, 1031–1032.
Stejskal, E. O., Schaefer, J. & MacKay, R. A. 1977 *J. magn. Reson.* **25**, 569–573.
Stark, R. E., Haberkorn, R. A. & Griffin, R. G. 1978 *J. chem. Phys.* **68**, 1996–1997.
Stockton, G. W., Johnson, K. G., Butler, K. W., Tulloch, A. P., Boulanger, Y., Smith, I. C. P., Davis, J. H. & Bloom, M. 1977 *Nature, Lond.* **269**, 267–268.
Waugh, J. S., Maricq, M. & Cantor, R. 1978 *J. magn. Reson.* **29**, 183–190.

PHILOSOPHICAL TRANSACTIONS OF THE ROYAL SOCIETY B BIOLOGICAL SCIENCES